Geometric Distortion Correction on EPI: An Application for Diffusion Tensor Imaging of the Human Optic Nerve

U. Techavipoo[1,2], A. Okai[2], T. Leist[2], A. Dresner[3], J. Lackey[1], J. Shi[1], and S. Lai[1]

[1]Radiology, Thomas Jefferson University, Philadelphia, PA, United States, [2]Neurology, Thomas Jefferson University, Philadelphia, PA, United States, [3]Philips Medical Systems, Best, Netherlands

Introduction:

The optic nerve is a pure white matter tract that is part of the central nervous system is often symptomatically involved in patients with multiple sclerosis (MS). As an isolated structure with defined fiber architecture, it provides the opportunity to study the effects of focal inflammation and demyelination on structural integrity. Diffusion tensor imaging (DTI) allows *in human* assessment of the microstructural architecture of the optic nerve. DTI requires several images with different directions of the diffusion-weighted gradients, and therefore, it generally utilizes echo-planar imaging (EPI) for fast acquisitions. However, EPI suffers from geometric distortion caused by susceptibility-induced magnetic field inhomogeneity from bone cavities and sinuses around the optic nerve. Our geometric distortion correction method that was presented last year [1, 2] was applied to suppress the distortion. A conventional DTI sequence was tailored practically to overcome difficulties such as the size of the optic nerve, the confounding signals from surrounding fat and cerebrospinal fluid (CSF), and the persistent motions from the eye movements. Values of DTI parameters before and after geometric distortion correction were compared to observe the integrity of the DTI sequence and the distortion correction.

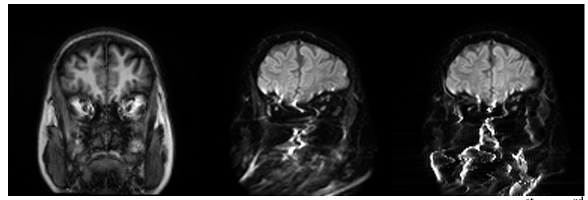

FIG. 1: T1WI, distorted T2WI, and corrected T2WI (from 1st to 3rd columns) using the proposed algorithm.

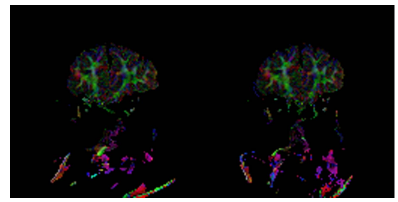

FIG. 2: Color-coded FA maps before (left) and after (right) distortion correction.

Materials and Methods:

Nine subjects with varying degrees of functional recovery from unilateral optic neuritis were participated in the studies. These subjects were classified into three groups: normal controls (NC), good visual recovery (GR), and poor visual recovery (PR). The results from each group were also divided into left (L) and right (R) eyes for NC and affected (A) and unaffected (U) eyes for GR and PR. The measurements were performed using a 3T MR scanner with an eight-channel head coil (Achieva, Philips Medical Systems, Best, The Netherlands). A DTI and field-mapping sequences using single shot spin-echo EPI were acquired in the coronal plan. The pixel size was set to 1.5×1.5 mm with 192-mm FOV and 3-mm slice thickness. Fat suppression was achieved using a standard STIR sequence. Inversion recovery was also used for CSF suppression with TI = 2500 ms and TR > 7000 ms. Parallel imaging using SENSE with P = 2.5 was also applied. The data were acquired in 2 packages (one for odd slices and the other for even slices) to maximize the recovery time (i.e., minimize the interference) between consecutive slices. Because for very long TR, multiple slices were allowed to acquire in between the TR to increase the efficiency. Therefore, the entire brain volume could be scanned without significant increase of the total scan time. For DTI, a b-factor of 850 s/mm^2 and 32 diffusion-weighted (DW) directions were used. Around 60 slices could be achieved in 9 minutes, and only 5 minutes if 15 DW directions were used. For the field mapping [1, 2], the parameters were similar to the DTI parameters, except that there was no DW image. Five dynamic images with −2 to 2 additional blips to generate 4 phase-shift maps for averaging were used in our experiments, and the acquisition time was around 2 minutes. In addition, standard T1-weighted images (T1WIs) were acquired as for anatomical reference. While scanning, the subjects were staring at a fixation point. However, they were allowed to blink but had to return to stare at the fixation point immediately afterward. All images were acquired under a software patch created to use inside our lab. Since the images after geometric distortion correction were easy to register to the T1WIs, ROIs slightly larger than the optic nerve were defined manually on T1WIs and then transferred to the corresponding DTI images. For images without correction, the ROIs were defined manually on the distorted T2-weighted images (T2WIs) from the DTI data. The DTI image pixels inside the ROIs were also trimmed using thresholds to eliminate the background noise. The thresholds were selected by comparing histograms of the pixel values of the T2WIs. Fractional anisotropy (FA), mean diffusivity (MD), principal eigenvalues (λ_1), and orthogonal eigenvalues (λ_{23}) were calculated and compared.

TABLE 1: MEAN VALUES AND THEIR STANDARD DEVIATIONS OF DTI PARAMETERS MEASURED BEFORE GEOMETRIC DISTORTION CORRECTION

Subject	FA	MD	λ1	λ23
NCR	0.47 ± 0.063	1339 ± 229	2026 ± 226	995 ± 232
NCL	0.52 ± 0.086	1313 ± 343	2062 ± 413	938 ± 313
GRA	0.37 ± 0.06	1405 ± 797	1992 ± 174	1111 ± 585
GRU	0.44 ± 0.043	1308 ± 153	1936 ± 153	993 ± 153
PRA	0.26	1475	1883	1271
PRU	0.41	1427	2052	1114

Note that MD, λ1, and λ23 units are in 10^{-6} mm^2/s.

TABLE 2: MEAN VALUES AND THEIR STANDARD DEVIATIONS OF DTI PARAMETERS MEASURED AFTER GEOMETRIC DISTORTION CORRECTION

Subject	FA	MD	λ1	λ23
NCR	0.50 ± 0.072	1144 ± 135	1759 ± 174	836 ± 135
NCL	0.47 ± 0.091	1166 ± 288	1751 ± 388	874 ± 259
GRA	0.39 ± 0.049	1397 ± 756	2022 ± 190	1084 ± 250
GRU	0.40 ± 0.028	1336 ± 111	1916 ± 132	1047±101
PRA	0.21	1449	1753	1296
PRU	0.3	1553	1999	1331

Note that MD, λ1, and λ23 units are in 10^{-6} mm^2/s.

Results:

Examples of T1WI, T2WIs before and after geometric distortion correction are shown in Fig. 1. The corresponding color-coded FA maps are shown in Fig. 2. As can be seen, after correction, the T2WI geometry is very compatible with the T1WI. The mean values of FA, MD, λ_1 and λ_{23} of the optic nerve were calculated across subjects on approximately 15 mm of the optic nerve immediately after the globes. These values before and after geometric distortion correction are shown in Tables 1 and 2, respectively. Note that the first 2 letters in subject names indicate the groups (NC, GR, and PR) and the third letter indicate the eye types (R and L, or A and U). For the NC group, these values are similar to those reported in [3]. The FA values from the right and the left optic nerves before and after correction are similar. However, the MD, λ_1, and λ_{23} values are lower after correction in mean but their standard deviations are still overlapped. For the GR group, all the values before and after correction are similar. The all values from affected and unaffected eyes are also similar. However, the FA mean values are around 10% lower than those in the NC group. However, their standard deviations still overlap. The MD values for this group are close to those reported in [4]. For the PR group, we have only one subject and therefore, the results are inconclusive. However, the results showed that the FA value from the unaffected eye is approximately 40% lower than that from the NC group, and the FA value from the affected eye is approximately 60% lower than that from the NC group.

Discussion and Conclusions:

We have shown that the DTI parameters before and after distortion correction are very similar. However, the geometry of the DTI images is matched to the anatomical reference image, resulting in better registration. The values of DTI parameters are comparable with those in the literature. The acquisition time for DTI measurement is practical, i.e., only 11 minutes (including the field-mapping scans) for the entire brain with 32 DW directions. If the number of DW direction reduces to 15, the total acquisition will be only 7 minutes. Since the entire brain is scanned, it is possible to combine the optic nerve study with other brain DTI studies. However, this method is sensitive to the positions of patients between the measurement and the field-mapping scans.

References:

[1] Techavipoo U., et al., ISMRM, p. 983, 2007. [2] Techavipoo U., et al. ISBI, p. 125-128, 2007. [3] Wheeler-Kingshott, C.A.M., et al., MRM, vol. 56, pp. 446-451, 2006. [4] Hickman, S. J., et al., AJNR, vol. 26, pp. 951-956, 2005.